UCRL-84282
PREPRINT

ALPHA PARTICLE CONFINEMENT IN TANDEM MIRRORS

R. S. Devoto
M. Ohnishi
J. Kern
T. T. Woo

This paper was prepared for publication in the Proceedings of the Fourth ANS Topical Meeting on the Technology of Controlled Nuclear Fusion, Valley Forge, PA, October 14-17, 1980.

October 10, 1980

ALPHA PARTICLE CONFINEMENT IN TANDEM MIRRORS*

R.S. Devoto, M. Ohnishi[†]
Lawrence Livermore National Laboratory, University of California
Livermore, California, USA 94550
John Kerns, J.T. Woo
Rensselaer Polytechnic Institute,
Troy, New York, USA 12181

Summary

Mechanisms leading to loss of alpha particles from non-axisymmetric tandem mirrors are considered. Stochastic diffusion due to bounce-drift resonances, which can cause rapid radial losses of high-energy alpha particles, can be suppressed by imposing a 20% rise in axisymmetric fields before the quadrupole transition sections. Alpha particles should then be well-confined until thermal energies when they enter the resonant plateau regime. A fast code for computation of drift behavior in reactors is described. Sample calculations are presented for resonant particles in a proposed coil set for the Tandem Mirror Next Step.

Introduction

In studies of tandem mirror reactors, it is generally assumed that the bulk of alpha-particle kinetic energy is transferred to the fuel ions and electrons, the alpha particles being lost when they reach thermal energies. Since they are initially only magnetically confined, a fraction is born in the loss cone and lost in a transit time. This fraction is

$$f \simeq \frac{1}{2R}$$

where R is the ratio of the maximum B field to the field in the central cell. The maximum field will generally be the plug mirror field but could be the outer field in an outer thermal barrier configuration. For typical conditions $f \simeq 10$-15%.

Some of the alpha particles will scatter into the loss cone as they drag down in energy. However, this fraction should be small since the drag time $\tau_d \simeq 1$s is much shorter than the 90° scatter time ($\tau_1 \simeq 200$ s at 3.5 MeV and 2 s at 350 keV).

When the alpha particle energy [illegible] $2\Phi_i$, where Φ_i is the center cell ion confining potential, then axial confinement follows the Pastukhov relation.[1] For the case $r_\alpha \ll R$, letting [illegible], and [illegible] we find

$$\frac{\tau_\alpha}{\tau_i} \sim \frac{M_i}{Z_\alpha M_\alpha} \; [illegible] \; (Z_\alpha - 1)\Phi_i/T_i \; [illegible]$$

For $\Phi_i = 2.5\ T_i$, typical of tandem mirror reactors, we find that thermal alpha-particles are confined better than [illegible] by factor [illegible] and to prevent build up of ash, the bulk of the alpha particles must be [illegible].

Mechanisms for radial losses in the [illegible] in tandem [illegible] have been identified [illegible] Ryutov and Stupakov.[2] The [illegible] involve particles which drift [illegible] multiples of [illegible] the other, the [illegible] resonant particles. The locations of the [illegible] depend [illegible] model [illegible] [illegible] [illegible] [illegible] [illegible].

Three types of [illegible] the presence of resonances: resonant banana, in which ions have adequate time to trace out bananas before collisions, resonant plateau, where banana orbits are interrupted by collisions before completion, and stochastic diffusion, which arises when resonant ions [illegible] large enough radial deflection on each reflection to move them to another resonance surface. [illegible] consideration of the [illegible] of these different mechanisms to [illegible] particle transport is given in the second section.

These initial considerations show that it is desirable to compute trajectories of alpha particles in actual reactor fields. We describe results of such calculations employing the long-thin approximation to the magnetic field. Both

*Work performed under the auspices of the U.S. Department of Energy by the Lawrence Livermore National Laboratory under contract number W-7405-ENG-48.

†Permanent address: Institute of Atomic Energy, Kyoto University, Uji, Kyoto, Japan.

$\underset{\sim}{E} \times \underset{\sim}{B}$ and finite-b effects are included. Some typical results are presented in the last section.

Alpha-Particle Resonances

The condition for resonance are

$$|\Delta\psi| = k/2 \qquad k = 1,3,5,\ldots\ldots \qquad (1)$$

where $\Delta\psi$ is the amount of azimuthal drift between reflections. The condition $k = 0$ in Eq. (1) corresponds to non-resonant banana orbits.[2] If the center cell length L_c is much greater than the length of the transition section, the dominant drift for $|\Delta\psi| \gg 0$ is due to $\underset{\sim}{E} \times \underset{\sim}{B}$ and grad B in the central cell. We find

$$\Delta\psi = \frac{c}{v_{\parallel} B} \frac{\partial \Phi}{\partial r} + \frac{\varepsilon \sin^2\theta}{ze B} \frac{dB}{dr} \qquad (2)$$

In order to proceed further, we must adopt a plasma model. We assume uniform electron and ion temperatures and utilize the long-thin approximation relating vacuum fields, B_v, to true fields. It has been argued by Ryutov and Stupakov[2] that the rapid radial mixing of electrons in the plugs will ensure uniform T_e. The temperature of the fuel ions would be expected to vary with radius, although initial computations for TMX show little variation. For the density profile

$$n = n_0 f(x_0), \qquad x_0 = r/r_p \qquad (3)$$

we find

$$\Phi = T_e \ln f + \text{constant} \qquad (4)$$

and

$$B^2 = B_v^2 (1 - \beta_0 f) \qquad (5)$$

where β_0 is the plasma β at $r = 0$. For the function, f, we take a model suitable for a reactor

$$f = \exp(-x^4) \qquad (6)$$

yielding

$$\Delta\psi = -\frac{2.89 \times 10^{-4} M^{\frac{1}{2}} L_c x^2}{\varepsilon^{\frac{1}{2}} \cos\theta \; r_p^2 B_v (1 - \beta_0 f)^{\frac{1}{2}}} \left[T_e - \frac{\varepsilon \sin^2\theta}{2z} \frac{\beta_0 f}{(1 - \beta_0 f)} \right] \qquad (7)$$

with T_e and ε in eV, M the alpha-particle mass in units of proton mass, and other quantities in the SI.

To show the explicit form of the resonant curves for alpha particles, we can consider a particular device, the Tandem Mirror Next Step (TMNS), currently under study.[3] Representative parameters for this machine are given in Table 1.

Table 1. Representative Parameters for TMNS

$\beta_0 = 0.5$	$B_v = 3.5$T
$L_c = 30$ m	$r_p = 54$ cm
$T_i = 40$ keV	$n_0 = 1.4 \times 10^{14}$ cm^{-3}
$T_e = 10$ keV	
$B_m = 9.5$T	$R = 1.64$

Near the axis the resonant curves are confined to small values of $V_{\parallel}$ while at moderate radii resonances extend nearly to the loss cone. A sample of the resonant curves is shown in Fig. 1 for $r = 40$ cm. Thus, near the reactor axis, here the alpha-particle production rate is highest, it is unlikely that alpha-particles will be lost radially before reaching thermal energies. Whether or not the thermalized alpha particles will accumulate to densities sufficient to "poison" the reaction can be answered definitively only by diffusion computations which include both fuel and alpha ions.

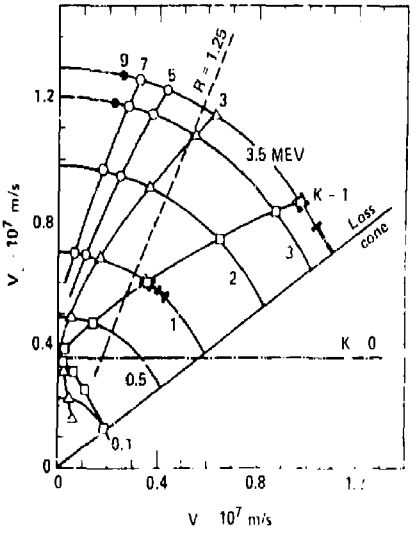

Fig. 1. Resonance curve for TMNS at $r = 0.4$ m. Modification of loss cone at low $V_{\parallel}$, $V_{\perp}$ due to electrostatic potential not shown. ⟨⟩ : numerically computed resonance width with $\underset{\sim}{E} \times \underset{\sim}{B}$ = grad $B = 0$ in transition section; ⟶ : numerically computed resonance width with all drift terms on.

The large number of resonances at moderate radii (Fig. 1) seem to indicate that radial losses could be substantial. However, the radial deflection on many of these resonances can be eliminated by a modest axisymmetric mirror before the quadrupole field rise.[4] The boundary for a mirror ratio of 1.25 is shown in Fig. 1. Essentially, all resonances with k > 1 are removed, i.e., have $\delta r = 0$. The mirror ratio corresponds to a lower value on mirror ratio when the axially uniform plasma pressure is taken into account. We find

$$R_v = R\left[1 - \beta_0 (1 - 1/R^2)\right]^{1/3} \qquad (8)$$

and

$$R_v = 1.11 \text{ for } R = 1.25 \text{ at } \beta_0 = 0.5.$$

It should be emphasized that the results of this section are strongly dependent on L_c. Larger values of L_c will cause all resonant curves to shift to higher values of $V_\parallel$, thus moving more resonances into the region where quadrupole effects are important. The transition between β-dominated and E x B dominated resonances depends only on T_e, β_0 and the assumed profile and will remain fixed in phase space.

Diffusion

Rvutov and Stupakov[2] suggest that high energy alpha particles would be in the stochastic regime where the diffusion coefficient is independent of collision frequency

$$D \sim (\delta r)^2 \epsilon^{1/2} \cos\theta / i_c \qquad (9)$$

The condition for stochastic diffusion is

$$\xi = \left|\frac{\delta r}{r}\right| r \left|\frac{\partial \chi \psi}{\partial r}\right| > 1 \qquad (10)$$

at a resonance. We can evaluate this expression from Eq. (7),

$$\xi = \left|\frac{\delta r}{r}\right| \frac{5.8 \times 10^{-4} M^{1/2} L_c x^2}{\epsilon^{1/2} \cos\theta r_p^2 B_v \sqrt{g}} \cdot$$

$$\left[\left(\frac{x^4 \beta_0 f}{g} - 1\right) T_e - \left(\frac{3 x^4 \beta_0 f}{g} - 1\right) \cdot \frac{\epsilon \sin^2\theta \beta_0 f}{2 Z g}\right] \qquad (11)$$

with $g \equiv 1 - \beta_0 f$.

In order to evaluate the criterion of Ineq. (10), we obtained values for $(\delta r/r)$ using a code[5] which computes guiding-center motion in a filament representation of the TMNS coils. Such calculations ignore the effect of finite β on field-line curvature in the transition section where the radial displacement takes place, but should give reasonable estimates of the magnitude of the displacement. The deflection δr for r = 40 cm is plotted vs $\epsilon_\parallel/\epsilon$ at ϵ = 3.52 MeV in Fig. 2 for a particular magnet design for TMNS (MAF/03B). We note a maximum $|\delta r/r|$ of about 0.140 occurring near the loss cone. The negative δr occurs because of the direction of the curvature vector at the end of the machine; rather surprising is the change in sign of δr (and also of the direction of azimuthal drift) near $\epsilon_\parallel/\epsilon$ = 0.4. This feature arises because the particular combination of axisymmetric and quadrupole fields for this design causes the curvature to change sign part way through the transition section. This particular magnetic field design also allows the quadrupole field to penetrate too far into the central cell, as reflected by the finite $\delta r/r$ for $\epsilon_\parallel/\epsilon \sim 0$. Calculations at other radii display the same behavior as Fig. 2; values for lower energy may be found from the scaling $\delta r/r \sim \sqrt{\epsilon}$.

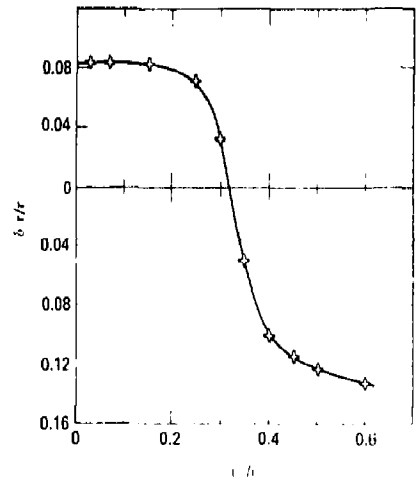

Fig. 2. Radial deflection per bounce for 3.52 MeV alpha particle in TMNS vacuum field vs $\epsilon_\parallel/\epsilon$.

From the curve in Fig. 2 and Eq. (11), we compute values for ξ as listed in Table 2. We see that stochastic diffusion should not be a problem for TMNS, providing a step in the axisymmetric field is introduced to eliminate the higher-k resonances. The criterion of Ineq. (10) is sensitive to L_c; raising L_c to 100 m, a typical value for a reactor could bring stochastic behavior for k = 3 and $\epsilon \gtrsim 3.5$ MeV.

The above scaling relation also applies to the resonant plateau regime. In the resonant

Table II. Values of for various resonances at 3.5 MeV

k	10 cm	20 cm	40 cm	60 cm
1	0.2	0.2	0.1	0.04
3	0.8	0.7	0.3	0.2
5	2.0	1.2	0.6	0.3
7	-	1.6	0.8	0.4

banana regime, the scaling is more favorable for alpha-particle confinement,

$$n \sim r^2(\delta r/r)^2 \epsilon^{-3/2} \qquad (12)$$

The latter is valid under the approximate conditions

$$v_\parallel > \frac{1.2 \times 10^{-12}\, n_i\, \Gamma_c}{|\delta r/r|^{3/2}\, \epsilon^{3/2}} \qquad (13)$$

Inserting appropriate numbers, we see that the alpha particles will be in the resonant banana regime until they thermalize when they will pass into the resonant plateau regime (fuel ions are also in this regime). Thus, even if only a very slight axisymmetric mirror is employed and several resonances remain, the alpha particles are expected to survive quite well to thermal energies.[6] Total alpha particle energy deposition fraction of 60-80% appears possible.

Equations of Motion

The guiding center equations of motion are given by

$$\frac{dv_\parallel}{dt} = \frac{-\mu \nabla B}{m} \cdot \hat{B} \qquad (14)$$

and

$$\underset{\sim}{v}_D = \frac{\underset{\sim}{E} \times \underset{\sim}{B}}{B^2} - \frac{\mu \nabla \underset{\sim}{B} \times \underset{\sim}{B}}{ZeB^2} + \frac{mv_\parallel^2}{ZeB} \hat{B} \times (\hat{B} \cdot \nabla)\hat{B} \qquad (15)$$

where μ is the magnetic moment and $\hat{B} \equiv \underset{\sim}{B}/B$. The axial electric field is neglected because the axial potential is small compared to the alpha particle energy. The parallel speed can be computed using conservation of energy and neglecting small terms. The parallel velocity is then obtained by changing the sign of $v_\parallel$ at each reflection. Therefore, Eq. (14) is replaced by

$$v_\parallel = \pm \sqrt{c - \frac{2\mu B}{m} - ze\phi} \qquad (16)$$

To solve Eqs. (15) and (16), we use a fourth order predictor-corrector technique.[7,8] It was previously observed[7] that particles can become stuck at the turning point of a Tokamak banana orbit in this algorithm. We observed similar problems in the tandem mirror. A barely trapped particle, i.e., one with pitch angle near the loss cone, could forget to turn and continue out of the machine. On other occasions, the particle would oscillate axially near the turning point as if it were caught in a field ripple and drift radially out of the machine. We circumvented this problem by anticipating slightly the turning point by monitoring the quantity

$$v^{*2} = v_\parallel^2 - \delta\, v_{TOT}^2$$

where v_{TOT} is the initial total speed and δ is a small quantity $\simeq 10^{-5}$. If v^{*2} becomes negative, in the predictor or corrector step, the step is stopped, the sign of $v_\parallel$ is changed and the predictor step restarted in the new direction. This turning criterion should be used only once per bounce but the particle may find itself beyond the mirror point and several time steps may be necessary before $v_\parallel^2$ becomes positive.

In order to make the drift equation tractable with finite pressure and perpendicular electric fields, we make the same assumptions as in the previous sections, i.e., Eqs. (3), (4) and (6) with Eq. (5) modified to

$$B = B_v \left[1 - \beta_0 \left(\frac{B_0}{B_v}\right)^2 \left(\frac{r_0}{r_p}\right)^4\right]^{\frac{1}{4}} \qquad (17)$$

and

$$\nabla B = \frac{B_v}{B} \nabla B_v + \frac{\mu_0}{B} p_{\perp 0} \nabla f\left(\frac{r_0}{r_p}\right) \qquad (18)$$

where r_0 is the field-line radius in the central cell where the vacuum field is B_0 and $p_{\perp 0}$ is the center line pressure there.

For the vacuum field we use the long-thin approximation which gives[9]

$$B_x = -(x/2)(f' - g'f) \qquad (19a)$$

$$B_y = -(y/2)(f' + g'f) \qquad (19b)$$

$$B_z = f(z) \qquad (19c)$$

where $f(z)$ and $g(z)$ specify the axial dependence of the axisymmetric and quadrupole fields on z. The two functions are found as cubic spline fits to the actual magnetic field with the aid of the additional information that the ellipticity of the flux tube cross section is $\exp[g(z)]$. The magnetic flux obeys the relation

$$\psi = \pi\left[x^2 e^{-g(z)} + y^2 e^{g(z)}\right] f(z) = \pi f(0) r_0^2 \qquad (20)$$

A last assumption involves the curvature terms. It is assumed that at any location the field direction is unchanged by finite pressure. This is equivalent to neglecting changes of the

curvature in the transition section. With the relation $\nabla \times B_v = 0$, the curvature term in Eq. (15) is reduced to

$$\hat{B} \times (\hat{B} \cdot \nabla)\hat{B} = \hat{B} \times \nabla \hat{B}_v .$$

The final expression for the drift velocity is

$$\underline{V}_D = \left[\frac{\mu}{2Ze}\ \frac{\beta}{1-\beta} - \frac{T_e}{B}\right] \frac{2}{\psi} \left(\frac{r_0}{r_p}\right)^4 \hat{B} \times \nabla\psi$$

$$+ \frac{m(1-\beta)^{\frac{1}{2}}}{Ze\ B^2} \left[\epsilon - Ze\phi - \frac{\mu B}{m}\left(\frac{1-2\beta}{1-\beta}\right)\right] \hat{B} \times \nabla B_v \quad (21)$$

where

$$\beta = \beta_0 \left(B_0/B_v\right)^2 \left(r_0/r_p\right) .$$

Results

The code described in the previous section has been used to compute drift surfaces for alpha particles at several different energies, pitch angles and radii in the TMNS field. As an example we show results for ϵ = 3.52 MeV, k = 1 resonance (θ = 35.1°), r_0 = 40 cm in Figs. 3 and 4. For this case β_0 = 0.50 and both grad B and E x B drifts are included in the central cell as well as the transition sections. Figure 3 shows x-z, y-z, y-x and r-z projections of the trajectory. The star shape in the y-x plot reflects the two "fans" in the transition sections rotated by 90° from one end to the other. The hollow portions at the ends of the x-z and y-z plots show that the angular deflection is approximately 90° per bounce. This observation is reinforced in Fig. 4 which shows the intersection of the drift surfaces with the midplane (z=0) of the center cell. The + and - symbols correspond to successive crossings of the midplane and are rotated by 90°. The banana shapes reminiscent of Tokamak orbits are evident. For this case $\Delta R/r$ = 0.19 and $\Delta R/\rho$ = 1.3 where ΔR is the maximum banana width and ρ is the alpha-particle Larmor radius.

As a check on the simple model of Section II, we have carried out equivalent calculations to locate the k=1 resonance for $\underline{E} \times \underline{B} = \text{grad } B = 0$ in the transition section. The resonance occurs over a finite width in θ as shown in Fig. 1 for ϵ = 1, 3.52 MeV. We note good agreement with the simple theory of Section II. Inclusion of grad B and E x B drift in the transition section shifts the resonance to lower values of θ and also increases the width $\Delta\theta$ of the resonance region as also indicated in Fig. 1.

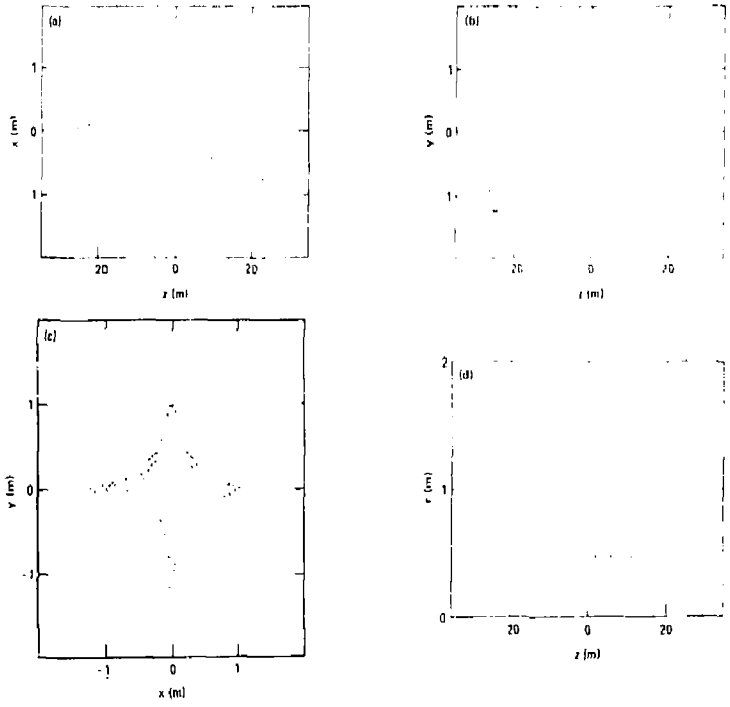

Fig. 3. Trajectory of alpha-particle guiding center in TMNS field for ϵ = 3.52 MeV. a: x vs z; b: y vs z; c: y vs x; d: r vs z.

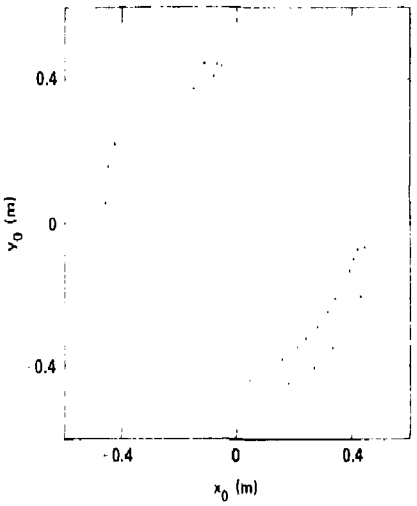

...ection of drift surface with TMNS ...e showing bananas. + and - cor... ...on to ions traveling in opposite di...ections.

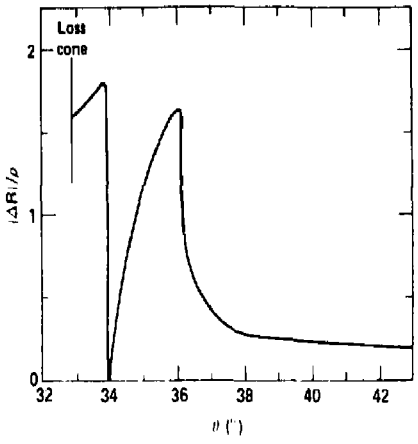

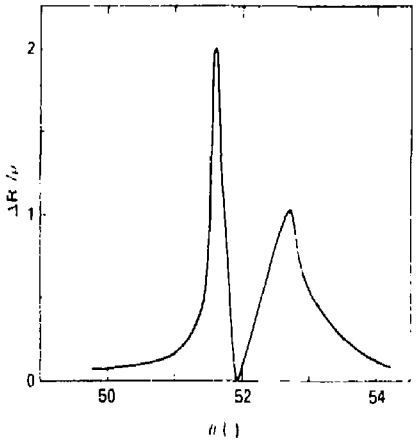

Fig. 5. Resonance width $|\Delta R|/\rho$ (ρ = ... radius) vs pitch angle for k = 1 resonance. a: $\mathcal{E}$ = 3.52 MeV; b: $\mathcal{E}$ = 1 MeV.

...e quantity $|\Delta R|/\rho$, where R is the maximum separation of inner and outer drift surfaces, is plotted for the k=1, resonance vs pitch angle θ in Fig. 5a ($\mathcal{E}$ = 3.52 MeV) and Fig. 5b ($\mathcal{E}$ = 1 MeV) for $\tilde{E} \times \tilde{B}$ and grad B drifts turned on in the transition section. The lower energy resonance is both narrower in $\Delta\theta$ and wider in $|\Delta R|$. It will be interesting to see if this trend continues to lower energy.

Surprising at first glance is the occurrence of $\Delta R = 0$ near the middle of the resonance region. This behavior can be explained by observing some of the midplane drift surfaces corresponding to Fig. 5a. In Fig. 6a, showing $|y_0|$ vs $|x_0|$ for $\theta = 33.3°$, we see what appears to be a banana. Actually it is not a banana but rather two widely separated drift surfaces. Particles are deflected from one to the other on each reflection. As θ is increased to 33.9°, a bulge starts to form on the outer drift surface (Fig. 6b) and with further increase in θ the bulge closes and becomes a banana. Near $\theta = 34°$, the banana becomes of vanishing ΔR and then expands again to the banana of Fig. 5a. An increase to $\theta = 36.9°$, the two drift surfaces reappear (Fig. 6c) and becomes of negligible separation with further increases in θ until the vicinity of the k = 3 resonance.

Concluding Remarks

The above results show that while confinement of ... substantial portion of alpha particle energy is probable, providing the magnetic field is correctly designed, it is desirable to actually compute loss rates as these ions thermalize. Such studies are currently underway.

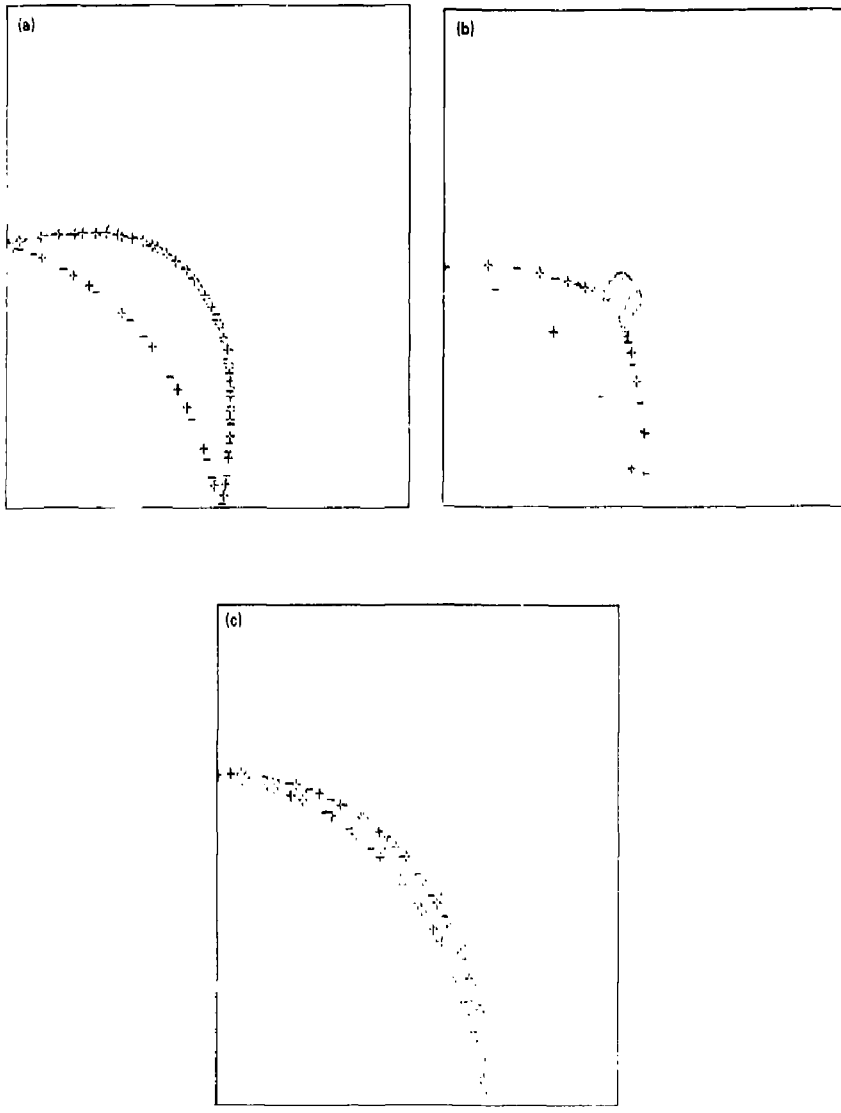

Fig. 6. Intersection of drift surfaces with midplane for k = 1, ε = 3.52 MeV.
a: θ = 33.3°; b: θ = 33.9°; c: θ = 36.9°.

REFERENCES

1. R.H. Cohen, M.E. Rensink, T.A. Cutler and A.A. Mirin, Nucl. Fusion 18, 1229 (1978).
2. D.D. Ryutov and G.V. Stupakov, JETP Letters 28, 174 (1977); Sov. Phys. Dokl. 23, 412 (1978).
3. J.N. Doggett et al., this meeting.
4. D.E. Baldwin, LLL UCID 17926 (1978).
5. R.S. Devoto (unpublished).
6. R.H. Cohen, Comm. Plasma Phys. 4, 157 (1979).
7. T.H. Johnson, LLL UCRL 51725 (1974).
8. C. Tull, LLL UCRL 52436 (1978).
9. J.C. Riordan, A.J. Lichtenberg, M.A. Lieberman, Nuclear Fusion 19, 21 (1979).